ENERGY GEOSTRUCTURES: A REVIEW ON THEIR ENERGY AND GEOTECHNICAL PERFORMANCE

Lyesse Laloui[1] and Melis Sutman[2]

KEYWORDS

Energy geostructures, Renewable energy, Thermo-mechanical, Design, Application.

ABSTRACT

Energy geotechnology provides low carbon, cost-effective and local energy solutions to structures and infrastructures, which opens a new era for the geotechnical engineering practice, by extending the conventional role of structural design to the one of addressing acute energy challenges of our century. The paper initially goes over the idea behind energy geotechnology by highlighting its scope and applications to various geostructures for structural support and energy supply of built environments. Aspects of primary importance for maximizing the energy, geotechnical and structural performance of energy geostructures and solutions to address this challenge are presented. Moreover, analytical solutions and design tools, as well as performance-based design of energy geostructures are introduced. The goal of this paper is to uncover the great potential of energy geotechnology on the path of less dependency on fossil fuels and to emphasize the new critical role of geotechnical engineers to take full advantage of this technology.

1. INTRODUCTION

The residential sector was responsible for 25.8% of final energy consumption in Europe in 2022, of which space heating and hot water production represented 78.4% in total (Eurostat, 2022), leading to around 2 400 Mt of direct CO2 emissions and 1 700 Mt of indirect CO2 emissions (IEA, 2022). Fossil fuel based and conventional electric equipment still dominates the global building market, accounting for more than 60% of space heating (IEA, 2022). Moreover, due to global warming, economic growth and urbanization, cooling is the fastest growing use of energy in buildings (IEA, 2018), which is mainly

[1] Laboratory of Soil Mechanics, Swiss Federal Institute of Technology Lausanne (EPFL), Lausanne, Switzerland
[2] Institute for Infrastructure & Environment, University of Edinburgh, Edinburgh, UK

covered by electricity. Without action to address energy efficiency, energy demand for space cooling will more than triple by 2050 (IEA, 2018).

Several initiatives and policies at national and international levels are being established in the construction sector (ASHRAE, 2008 and European Directive 2010/31/EU, 2010) for the implementation of zero- or nearly zero-energy buildings. For instance, ASHRAE Vision (2008) presents requirements to enable buildings to produce as much energy as they use by 2030. On the other hand, European Directive 2010/31/EU (2010) requires all new public buildings to be nearly zero-energy by 2018 and all new buildings by the end of 2020. Therefore, the development and the diffusion of reliable, eco-nomically viable and environmental-friendly technologies to satisfy a noteworthy part of the energy needs of the building sector is an important challenge.

Conceptually, energy geostructures is a technology enabling the use of renewable energy sources for efficient space heating and cooling. In this technology, any geo-structure in contact with the soil and already required for structural support are equipped with geothermal loops, for heat exchange operations to exploit the near surface geothermal energy. The idea behind energy geostructures comes from the fact that the temperature of the ground remains the same throughout the year below a depth of 6-8 meters. Therefore, with the integration of the geothermal loops and the water-antifreeze mixture circulating within them, the heat is extracted from the ground to heat the buildings during winter. Similarly, during summer, the extra heat coming from the building side is injected into the ground to cool them. In this system, ground source heat pumps (GSHP) are often required which works intermittently in order to adapt the temperature of the circulating fluid to meet the energy demands from the building side.

The heat energy that can be provided by the energy geostructures depends on various factors, including, but not limited to, the thermal and hydraulic properties, and mean temperature of the ground, geothermal and geotechnical design of the geo-structures, and the energy demand from the building side. However, 40-150 W/m, 20-40 W/m^2 and 20-60 W/m^2 are achievable energy extraction or withdrawal amounts from energy piles, energy walls and energy tunnels, respectively. As a practical example, a recent numerical investigation was performed at the Laboratory of Soil Mechanics (LMS), considering a five-storey office building, with net heated/cooled area of 2400 m^2, bearing on 32 piles with 0.5 m diameter and 20 m length which were used as energy piles. The results of the analysis show that the energy piles can supply 100% of the heating demands and most of the cooling demands of the office building in Sevilla, Spain. An auxiliary air conditioning system was required only during July and August, to provide the remaining 11% and 6% of the cooling demand (Sutman et al., 2019).

2. ENERGY ASPECT

Typical energy problem

Operation of energy geostructures to meet the heating and cooling demands from the building side involves heat exchange within the three components of the ground source heat pump system, being the primary circuit, the GSHP and the secondary circuit (Figure 1).

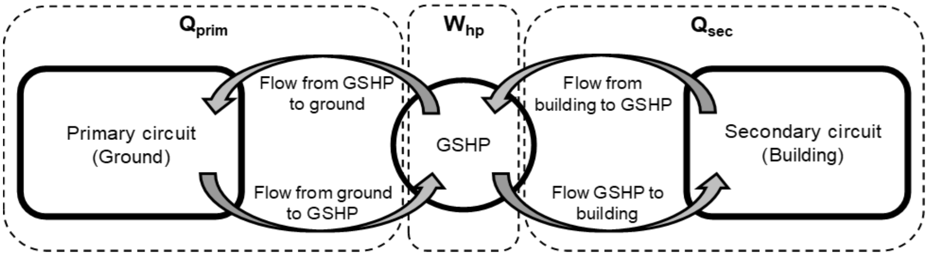

Figure 1 Heat exchange within three components of ground source heat pump system.

In the primary circuit, the heat exchange occurs between the ground and the GSHP, where the heat is extracted from or withdrawn into the ground for heating or cooling the building side, respectively. The heat exchange mechanism that occurs between the ground and the energy geostructure is shown in Figure 2, through the example of an energy pile, for both building heating and cooling purposes.

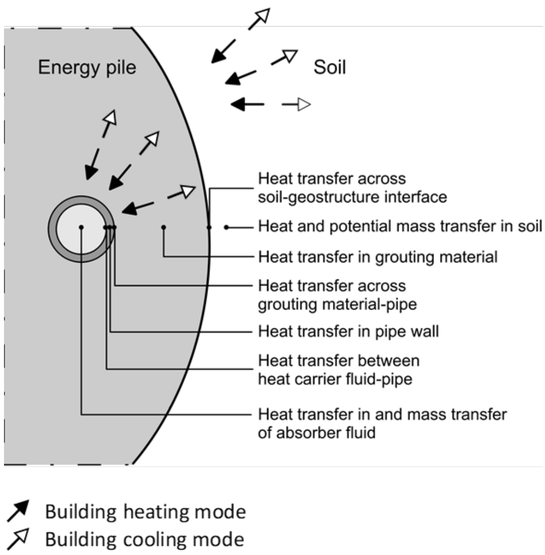

Figure 2 Heat exchange between the energy pile and the ground.

Regarding the building cooling mode, shown by the white arrows, the temperature of the circulating fluid returning from the building side is warmer than the ground temperature, which results in a thermal gradient. The circulating fluid exchanges heat with the ground loop wall through convection, which is followed by a heat conduction through the wall of the ground loop and the pile until reaching the pile-soil interface. Finally, the heat is transferred within the ground mainly by conduction and partially with convection if a moisture migration takes place. Similarly, during the building heating mode, the returning fluid temperature is colder than the ground temperature and the heat exchange occurs in the reverse direction, as shown by the black arrows.

Assuming pure thermal conductivity within the energy pile and the ground, the energy conservation equation reads:

$$\rho c \frac{\partial T}{\partial t} - div(\lambda \boldsymbol{grad} T) = 0 \qquad (1)$$

where ρ is the density, c and λ are the specific heat capacity and thermal conductivity, respectively, including both fluid and solid components, T is the temperature, t is the time and div and ***grad*** are the divergence and gradient operators, respectively. The energy conservation equation for the incompressible circulating fluid within the loops can be written as:

$$\rho_f A_p c_f \frac{\partial T_f}{\partial t} + \rho_f A_p c_f \boldsymbol{u_{f,i}} \cdot \mathbf{grad} T_f = \mathrm{div}\left(A_p \lambda_f \mathbf{grad} \mathrm{T}_f\right) +$$

$$\frac{1}{2} f_D \frac{\rho_f A_p}{d_h} |\boldsymbol{u}|^3 + q'_w \qquad (2)$$

where ρ_f, c_f, and λ_f are the density, specific heat capacity, and thermal conductivity of the fluid, respectively; A_p and d_h are the cross-sectional area and hydraulic diameter of the pipe, respectively; T_f is the temperature of the fluid; $u_{f,i}$ is the velocity vector; f_D is the Darcy friction factor; and q'_w represents the heat flux per unit length that is exchanged through the pipe wall.

In the secondary circuit, the heat is transferred to or from the building side for heating or cooling purposes, respectively. In between the two circuits, there exists the GSHP to transfer the heat between the two circuits. The efficiency of the GSHP is quantified by the coefficient of performance (*COP*) through examining the amount of energy input to operate the GSHP (W_{hp}) and the energy that can be supplied to the building side (Q_{sec}), as shown below:

$$COP = \frac{Q_{sec}}{W_{hp}} \qquad (3)$$

State of the Art on the Application of Energy Geostructures

To reveal the actual energy performance of energy geostructures, a comprehensive investigation was performed by incorporating information from (i) a survey targeting international construction companies involved in energy geostructures, (ii) available literature on operational energy geostructures and (iii) complementary results by Di Donna et al. (2017). Figure 3 presents the state of the art on energy piles, based on the integration of the information from 157 energy pile projects, in terms of extracted thermal power with respect to the diameter and length of the piles. On the other hand, Figure 4.a and Figure 4.b represent extracted and injected heat for heating and cooling purposes for energy walls (17 projects) and energy tunnels (11 projects), respectively.

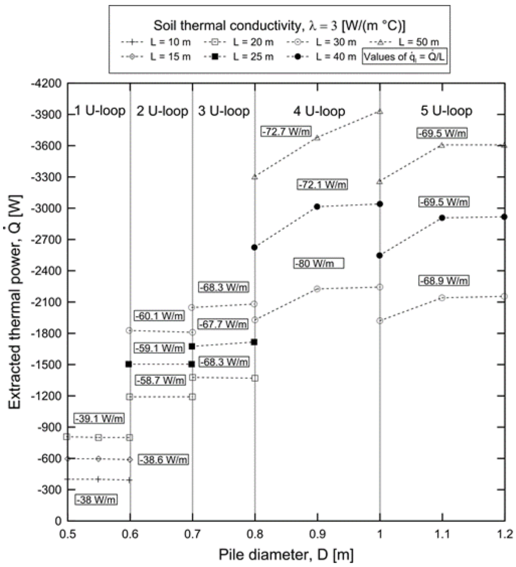

Figure 1 State of the art on application of operational energy piles (Laloui and Rotta Loria, 2019).

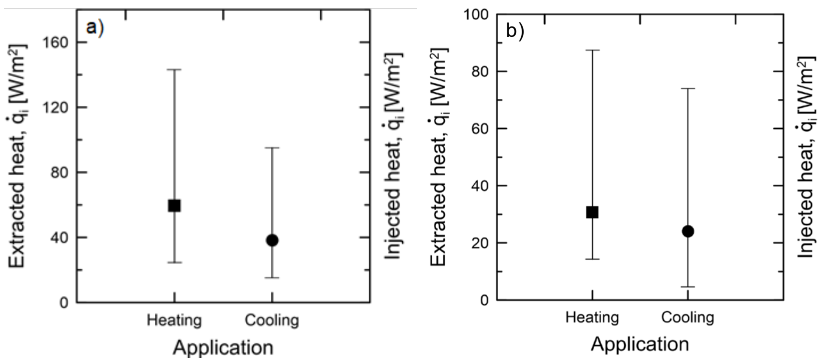

Figure 4 State of the art on application of energy walls and tunnels (Laloui and Rotta Loria, 2019).

3. GEOTECHNICAL ASPECT

As shown in the previous section, energy geostructures concept, a technology capable of exploiting geothermal sources for both space heating and cooling, is undoubtedly an outstanding candidate to cut down the governance of unsustainable resources. Yet, the use of conventional geostructures for heat exchange purposes is associated with temperature changes, hence thermal loads and displacements, along the geo-structures and within the surrounding soil, which needs to be taken into consideration in addition to the typical geotechnical design (Laloui and Sutman, 2021, Laloui et al., 2014).

In order to understand the extent of temperature change effects on energy geostructures, several in-situ tests were performed on single (Laloui et al., 2006; Bourne-Webb et al., 2009; You et al., 2016; Loveridge et al., 2016; McCartney and Murphy, 2017; Sutman, 2016; Sutman et al., 2017; Sutman et al., 2019) and a group of energy piles (Mimouni et al., 2015; Rotta Loria et al., 2016), energy walls (Xia et al., 2012) and energy tunnels (Adam and Markiewicz, 2009; Frodl et al., 2010; Nicholson et al., 2014; Barla et al., 2019). Moreover, several models or tools with varying complexity were developed for the analysis and design of energy piles (Knellwolf et al., 2011; Bourne-Webb et al., 2014; Salciarini et al., 2013; Rotta Loria and Laloui, 2016; Makasis et al., 2018, Sutman et al., 2018), energy walls (Kürten et al., 2015; Sterpi et al., 2017; Sailer et al., 2019) and energy tunnels (Barla and Di Donna, 2018; Bidarmaghz and Narsilio, 2018). The previous research answered the most fundamental questions on the mechanisms governing the thermal and structural behavior of energy geostructures. These efforts opened a new era for the geotechnical engineering practice, by extending the conventional role of geotechnical design to the one of addressing acute energy challenges of our century.

Full-Scale Experimental Analysis on Energy Piles

The two pioneering full-scale in-situ tests on energy piles performed at Swiss Federal Institute of Technology in Lausanne (EPFL), investigating (i) the response of a single energy pile to combinations of thermal and mechanical loads and (ii) the response of a group of closely spaced energy piles to thermo-mechanical loads are presented in this section. Compressive stresses and upward shaft resistance mobilization are considered positive, according to the adopted sign convention.

(i) Response of a Single Energy Pile to Combinations of Thermal and Mechanical Loads (Laloui et al., 2003):

A pioneering field test was performed at EPFL campus, on a single energy pile, with a diameter of 0.88 m and length of 25.8 m, under a newly constructed 5-storey building (Bâtiment Polyvalent). The single energy pile was one of the 97 bored piles constructed under the building. Along the test pile, polyethylene (PE) tubes were installed vertically on the reinforcing structure with a U-shaped configuration to permit the passage of the heat-carrying fluid. The test pile was instrumented by a considerable number of sensors to enable the measurement of temperature, strain and toe load variations during the thermal load applications.

The soil profile at the field test site consists of alluvial soil at the first 12 m (Layers A1 and A2) which is followed by a sandy gravelly moraine (Layer B) and bottom moraine (Layer C) until around 25 m. Finally, a molasse layer (Layer D) is found under the moraine. The ground water table at the test site is located at ground surface. Further information on soil and soil-pile interaction, as well as the test pile and instrumentation can be found in Laloui et al. (2003).

A heating and passive cooling cycle was applied to the test pile following the completion of each storey of the building with the purpose of evaluating the influence of structural load on the development of thermally induced axial stresses and displacements. Figure 5.a shows the results of the last test which was performed after the construction had been finalized. The distribution of the mechanical load profile shows the absence of toe resistance which implies that the structural load was entirely carried by the mobilized resistance along the shaft of the test pile. The following temperature increase, with a magnitude of 13.4˚C, resulted in generation of thermally induced compressive axial loads with a significant mobilization of the toe (2000 kN) and thermally induced axial loads at the pile head (1000 kN).

Shaft resistance mobilization due to mechanical and thermal loads along the same test pile is shown in Figure 5.b and Figure 5.c. The mechanical load application resulted in downward displacement of the pile which is associated with positive shaft resistance mobilization. The subsequent temperature increase caused the portion of the pile, above the null point, the depth at which no thermally induced displacement is observed, to possess an upward displacement, resulting in a decrease in corresponding shaft resistance mobilization due to mechanical and thermal loads along the same test pile is shown in Figure 5.b and Figure 5.c. The mechanical load application resulted in downward displacement of the pile which is associated with positive shaft resistance mobilization. The subsequent temperature increase caused the portion of the pile, above the null point, the depth at which no thermally induced displacement is observed, to possess an upward displacement, resulting in a decrease in corresponding shaft resistance (Figure 5.b). On the other hand, the portion below the null point displaced downward, further mobilizing the positive shaft resistance (Figure 5.c).

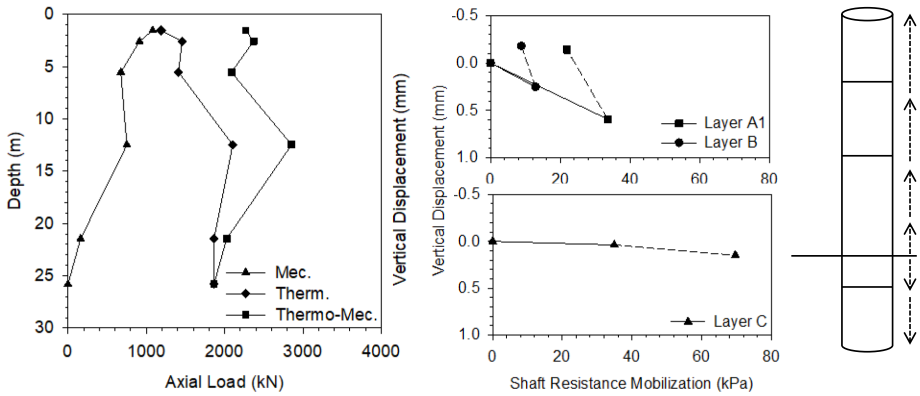

Figure 5 a) Mechanical, thermal and combined thermo-mechanical loads. b, c) Shaft resistance mobilization along the test pile.

(ii) Response of a Group of Closely-Spaced En-Ergy Piles to Thermo-Mechanical Loads (Mimouni and Laloui, 2015; Rotta Loria and Laloui, 2017)

A second field test was implemented at EPFL campus by equipping four out of 20 piles under a water retention tank within the Swiss Tech Convention Center to evaluate the thermally induced group effects among closely-spaced energy piles. The piles were 0.9 m in diameter and 28 meters in length. Each test pile was equipped with four 24 m long U-loops connected in series which were installed 4 m below the pile heads in order to prevent the thermal interaction with the water retention tank. The test piles were instrumented with vibrating wire strain gages at every 2 meters along the length, a pressure cell at the toe and radial optical fibers. Moreover, thermistors and piezometers were installed within boreholes at close proximity to the test piles to monitor the temperature and pore water pressure changes during the field test. The field test site is 200 m away from the single energy pile test location, resulting in similar stratigraphic characteristics (Mimouni and Laloui, 2015).

Heating with maximum temperature increase of 20˚C and passive cooling cycles were applied to single (EP1) and the group of four energy piles (EPall) (Rotta Loria and Laloui, 2017). Figure 6 shows (i) thermally induced axial strains and stresses along EP1 when serving as the only operating pile among the group of four piles (20EP1) and (ii) average thermally induced axial strains and stresses along the length of all four piles during full geothermal activation of the group (EPall). The comparison of tests 20EP1 and 20EPall shows that the presence of thermally induced group effects govern the higher development of axial strain when more energy piles operate as geothermal heat exchangers in a closely spaced pile group than when only one energy pile serves this purpose (Figure 6.a).

Figure 6.b shows the comparison in terms of thermally induced axial stresses where an opposite behavior was attained corresponding to a decrease in thermally induced axial stresses as the number of thermally active energy piles increases. This phenomenon is associated with the increased deformation of energy piles operating in a group (Figure 6.a) which results in lower thermally induced blocked strains, since the temperature change and hence the free thermal strains are the same for Test 20EP1 and 20EPall, and therefore lower observed axial stresses. Moreover, tensile stresses were observed at the bottom portion of the energy piles during test 20EPall, which is associated with the thermally induced deformation of the molasse layer resulting in a pull-down effect. This effect was less pronounced during the test 20EP1 since the compressive stresses induced by the restrained expansion of EP1 overcame the tensile stresses exerted by the surrounding molasse layer.

Comparison of thermally induced strains and axial stresses per unit temperature change corresponding to geothermal operation of a single energy pile (Test 20EP1) and a group of energy piles (Test 20EPall) is presented in Figure 7.a and Figure 7.b, respectively, which are average values along the active length of the piles. The figures clearly show greater average vertical strains and lower average axial stresses with increasing number of active energy piles. In terms of design aspects, analysis of a single pile in a closely-spaced group will lead to a conservative estimate of vertical stresses that can be employed during the preliminary design stages, but is not the case for the vertical strains.

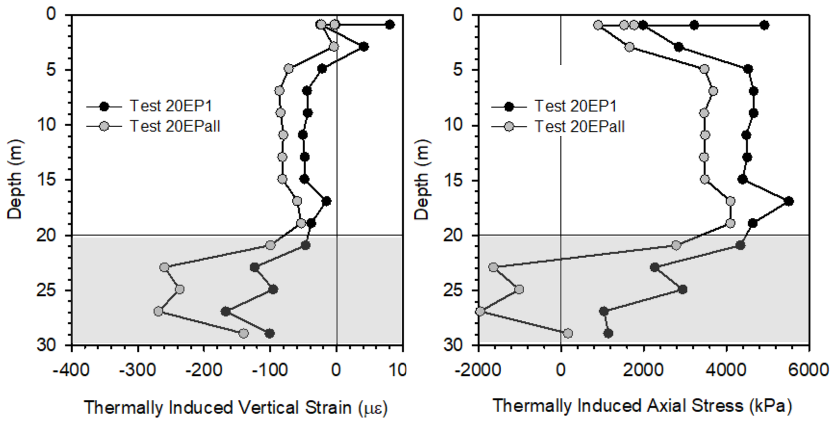

Figure 6 a) Thermally induced axial strains b) Thermally induced axial stresses during tests EP1 and EPall.

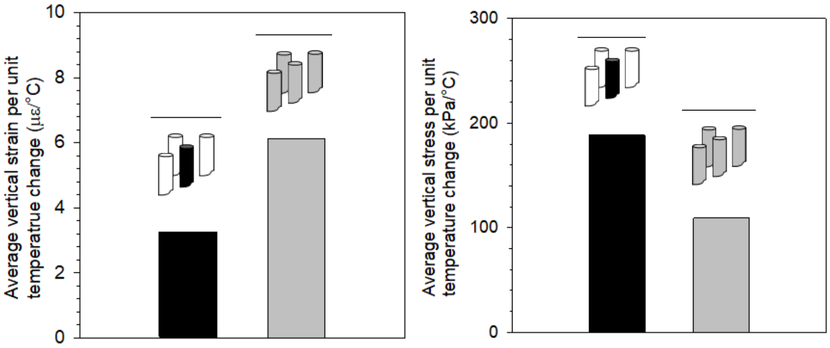

Figure 7 a) Thermally induced group effects in terms of a) Axial strains and b) Axial stresses (redrawn after Rotta Loria, 2019).

Analytical Methods for the Analysis of Energy Piles

Full-scale in-situ tests provided the most fundamental information regarding the response of a single and a group of energy piles to thermo-mechanical actions. Moreover, finite-element methods, the majority of which have been validated by the results of the in-situ tests, were developed, and are considered to be the most rigorous approach for the analysis of energy piles. However, these comprehensive methods require a considerable number of geotechnical parameters, as well as high computational efforts, which renders them more suitable for research purposes rather than for practical piling problems. For the design and wider application of energy piles, a reasonable balance between excessive complexity and unsatisfactory simplicity should be established for the development of practical analytical models. Therefore, several simplified analytical methods have been developed by the Laboratory of Soil Mechanics to serve as preliminary design guidance of single and groups of energy piles.

(i) Load-Transfer Approach for Single and Group of Energy Piles (Knellwolf et al., 2011; Ravera et al., 2020)

The load-transfer approach, where the soil-pile interaction is represented by springs distributed along the pile shaft and toe by neglecting the continuity of the soil domain, is one of the most common analytical methods employed for the analysis of conventional piles (Seed and Reese, 1957; Coyle and Reese, 1966). In this approach, numerous analytical and empirical methods have been proposed to define the load-transfer curves (Randolph and Wroth, 1978; Frank and Zhao, 1982; Kraft et al, 1981). Later on, considering that most piles are implemented in groups in practice, the load-transfer curves have been modified to consider group effects (Randolph and Clancy, 1993; Comodromos et al., 2016). Given the great potential of the load-transfer approach in providing a practical tool for the analysis of axial loaded conventional piles, the approach has been implemented for the analysis of single and groups of energy piles.

The load-transfer approach has first been modified for single energy piles by Knellwolf et al. (2011), where the pile is divided into rigid elements that are connected to each other and to the surrounding soil by the springs (Figure 8.a). In order to define the relationships between the mobilized shaft friction/toe resistance and displacement, the method from Frank and Zhao (1982) was utilized, relating the shaft and toe stiffness to Menard pressuremeter modulus and dividing the load-transfer curve into three main sections: (i) initial linear part characterizing the elastic response, (ii) second linear part associated with the elastoplastic response and (iii) final plateau referring to perfectly plastic response as represented in Figure 8.b by full lines for single isolated piles. The presence of a slab above energy piles was considered in a simplified way by introducing an additional spring linked to the pile head. The analytical model is validated by the results of both EPFL single pile in-situ test (Laloui et al., 2006) and Lambeth College in-situ test (Bourne-Webb et al., 2009) and has also been implemented in the Thermo-Pile Software developed by Laboratory of Soil Mechanics for the analysis and design of energy piles.

Following the same logical sequence as the one of conventional piles, the load-transfer approach for single energy piles has subsequently been extended to characterize the response of groups of energy piles to thermo-mechanical loads in a simplified, yet rational manner (Ravera et al., 2020). To represent the interaction between a group of energy piles, a displacement ratio (R_d) was introduced adapting the displacement response of a single isolated energy pile to the one of an energy pile in a group:

$$R_d = \frac{w_{gr}}{w_{is}} \quad (4)$$

Where w_{gr} is the average displacement of group and w_{is} is the displacement of a single pile subjected to same average load. As in the case of the approach proposed for conventional piles (Comodromos et al., 2016), the displacement ratio depends on the geometric configuration as well as the variations in the displacement field introduced by thermal and mechanical loads. In this approach, the ultimate shaft resistance of an energy pile in a group is considered to be the same as the one of a single isolated energy pile, while the displacement ratio is applied to adapt the displacement necessary to mobilize it. The load-transfer curve attained for a single energy pile in a group is represented by dashed lines in Figure 8.b and is determined as follows:

$$w_{gr} = R_d w_{is} \quad (5)$$

$$t_{s,gr} = t_{s,is} \quad (6)$$

where w_{gr} and $t_{s,gr}$ are the displacement and shaft resistance of an energy pile in a group, and wis and $t_{s,is}$ are the displacement and shaft resistance of a single isolated energy pile, respectively. The load-transfer curve in Figure 8.b is determined using the method proposed by Frank and Zhao (1982), yet, any method developed for single conventional piles can be employed provided that a displacement factor is applied. Finally, since the behavior of a pile in the group highly depends on its location, the displacement ratio may also be corrected by introducing a location weighting factor (Comodromos et al., 2016).

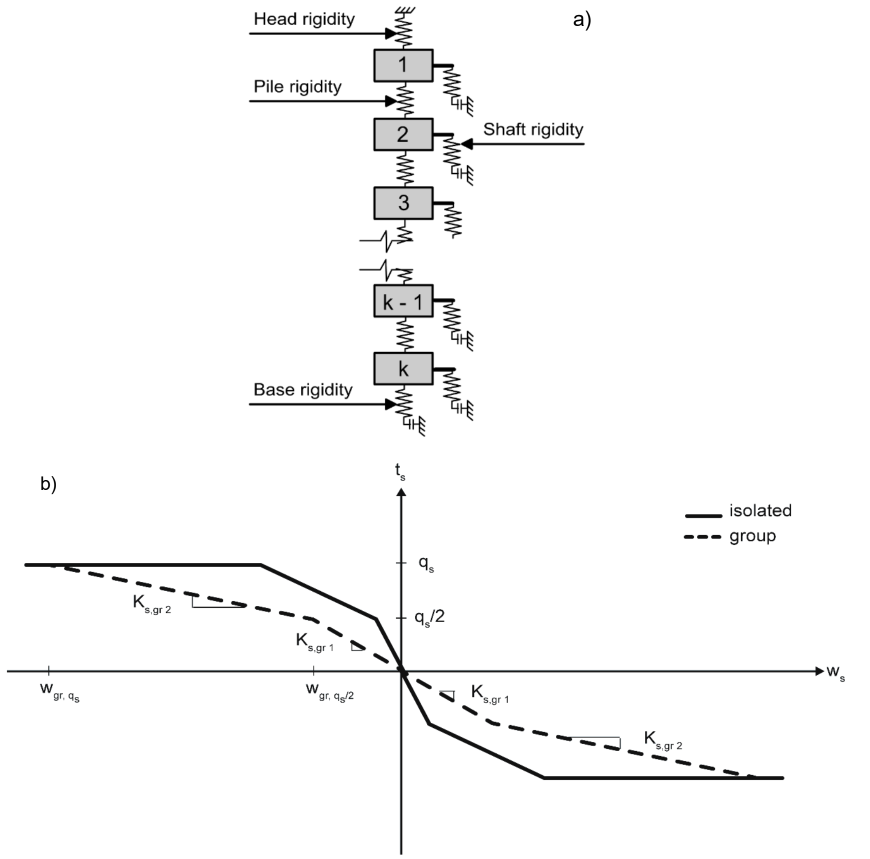

Figure 8 a) Modelling approach b) Load-transfer relationship for single isolated energy pile and energy pile in a group.

The proposed method has been implemented in Comsol Multiphysics Software and its competence in analyzing the behavior of a group of energy piles has been investigated through the results of the full-scale in-situ test performed at EPFL campus, on a group of four energy piles. The material properties considered in the analysis as well as the development of the load-transfer curves are explained in detail by Ravera et al. (2020). Comparison of experimental data from the full-scale in-situ test (Rotta Loria and Laloui, 2018) and the numerical results obtained through the implemented method is presented in Figure 9.a and Figure 9.b, in terms of thermally induced axial stress and mobilized shaft resistance, respectively at 20˚C temperature increase. The numerical results were attained employing two sets of parameters for the molasses layer in compliance with the ones presented in Knellwolf et al. (2011).

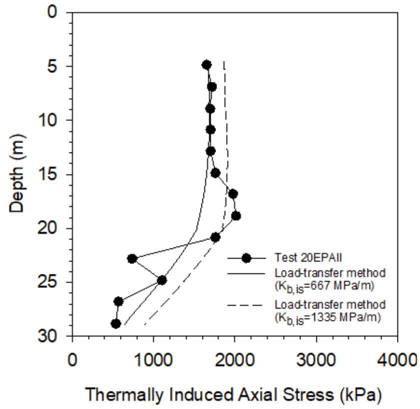

Figure 9 a) Comparison between experimental data and numerical results for a) Thermally induced axial stresses and b) Mobilized shaft resistance (redrawn after Ravera et al., 2020).

The comparison presented in Figure 9 corresponds only to the geothermal activation of the group of energy piles, excluding the stresses generated by the body load and structural loads. The stress variation corresponds to the average value of the mean temperature variations along the uninsulated portions of all four energy piles in the group and the mobilized shaft resistance is determined by employing the stress variations. A good agreement between the experimental and numerical results is observed in the figure, despite the simplifications inherent in the theory.

It was previously shown in Figure 7 that thermally induced vertical stresses decrease for the same temperature change as the number of geothermally active energy piles increases due to increased vertical strains caused by group interactions. The agreement between experimental and numerical results corroborates the additional value of this method, which allows determination of the thermally induced vertical stress along the depth of an energy pile in a group in a simplified and rational manner.

(ii) Interaction Factor Method for Group of Energy Piles (Rotta Loria and Laloui, 2016; Ravera et al., 2019)

A second analytical method was extended from the interaction factor method in the framework of conventional pile groups (Poulos, 1968) to the one of energy pile groups in order to provide a simplified yet rational analysis tool for estimating the vertical displacement of energy pile groups subjected to thermal loads (Rotta Loria and Laloui, 2016). The method allows the estimation of the head displacement of any energy pile in a group by employing the interactions between two energy piles and the superimposition of the individual effects of adjacent piles in the group as follows:

$$w_k = w_i \sum_{i=1}^{i=n_{EP}} \Delta T_i \Omega_{ik} \qquad (7)$$

where w_i is the vertical head displacement of a single isolated pile per unit temperature change, ΔT_i is the applied temperature change to pile i, and Ω_{ik} is the interaction factor for two piles corresponding to the center-to-center distance between pile i and k. Interaction factor charts, characterizing a group of two energy piles and taking into consideration pile slenderness ratio and spacing, pile-soil stiffness ratio, Poisson's ratio and non-uniform moduli of the soil have been developed to determine Ω_{ik} (Rotta Loria and Laloui, 2016).

The formulation above provides solutions regarding the displacement interaction for free standing energy pile groups or energy pile groups with a perfectly flexible slab. However, in practice piles are often rigidly attached to a pile cap which stands on the soil (Poulos, 1968). Therefore, it is essential to consider thermally induced mechanical interactions which are governed by the changes in deformation field, due to the interplay between the energy pile-slab-soil responses. With this purpose, the interaction factor method was further extended to take into account the presence of the pile cap (Ravera et al., 2019). 3D steady state finite element simulations were carried out employing Comsol Multiphysics Software to propose a formulation of the interaction factor for energy pile groups under a slab and to propose design charts for the analysis compatible with the former study. The influence of the rigid pile cap is expressed in terms of pile-cap displacement ratio as follows:

$$R_c = \frac{displacement\ of\ pile\ with\ cap}{displacement\ of\ free\ standing\ pile} \qquad (8)$$

Employing the pile-cap displacement ratio, displacement determined in free standing conditions can be adjusted to consider the contacting slab as follows:

$$w_k = R_c w_i \sum_{i=1}^{i=n_{EP}} \Delta T_i \Omega_{ik} \qquad (9)$$

The combination of the two methodologies (1) interaction factor method for free standing energy piles and (2) extension of the method to consider the presence of the slab yields the following ultimate methodology illustrated in Figure 10. The first three steps belonging to the original methodology (Rotta Loria and Laloui, 2016) and the following two steps corresponding to the extension of the method (Ravera et al., 2019), are as follows:

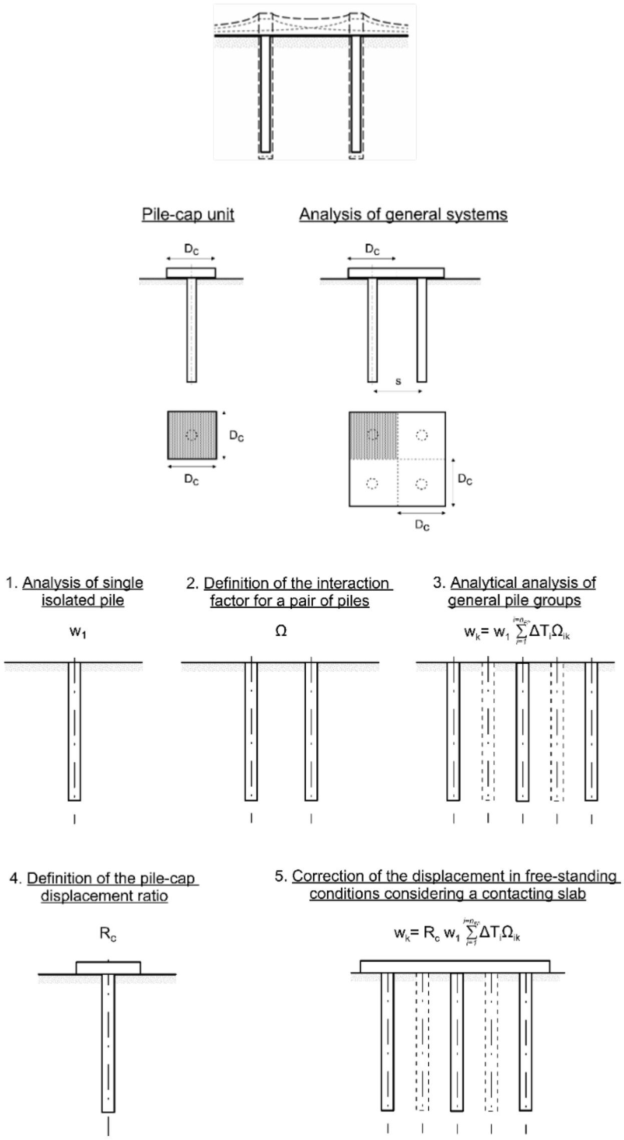

Figure 10 Steps of interaction factor method for the analysis of energy piles with contacting slab.

Step 1: Displacement of an isolated energy pile is computed by employing any suitable practical or sophisticated method as long as it returns representative displacement values for the considered case.

Step 2: Interaction factor is determined for a pair of two energy piles employing the design charts provided by Rotta Loria and Laloui (2016). A sample design chart regarding an energy pile with a slenderness ratio of twenty-five bearing in a soil with a Poisson's ratio of 0.3 is presented in Figure 11.a, for various soil-pile stiffness and normalized displacement.

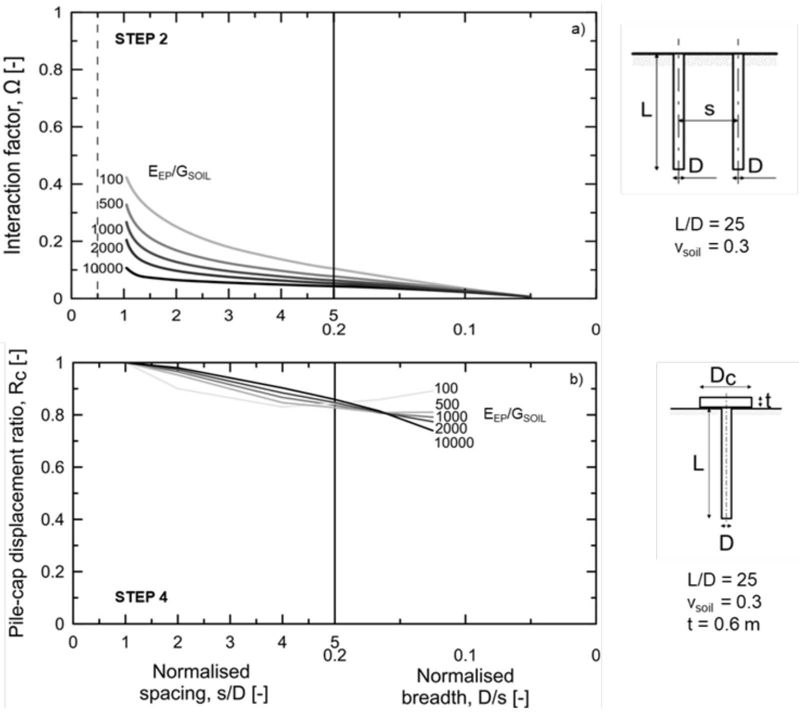

Figure 11 a) Interaction factors, b) Pile-cap displacement ratio for L/D = 25.

Step 3: Vertical head displacement of any pile in the group in free standing conditions is calculated employing Equation (7).

Step 4: Pile-cap displacement ratio is determined referring to the design charts presented by Ravera et al. (2019). A sample design chart, compatible with the one presented for Step 2, is shown in Figure 11.b for pile cap thickness of 0.6 m.

Step 5: Displacement determined in Step 3 for free standing conditions is corrected by employing Equation (9).

The rather approximate yet rational methodology presented above enables the estimation of the head displacement of any energy pile group configuration with a slab supported on soil through the displacement of a single isolated energy pile and superimposition of the individual effects of adjacent piles and the slab in the group, providing a practical tool to perform displacement analysis of energy pile groups in the early stages of the design process.

4. DESIGN OF ENERGY PILES

Full-scale in-situ tests that have been performed on energy piles, as well as the numerical and analytical tools that have been developed over more than two decades, revealed the most fundamental information leading to the recommendations regarding the design of energy piles. According to these findings the design of energy piles at ultimate limit states can be considered as a conventional process by considering that the reactions provided by the soil above and below the null point compensate for each other ensuring equilibrium and, provided that the structural elements are characterized by adequate ductility and rotation capacity (Rotta Loria et al., 2020). However, regarding the serviceability limit states, the effects of both mechanical and thermal loads should be examined by taking into consideration the vertical displacement of single and group of energy piles, as well as the deflection or angular distortion.

Regarding the combinations of actions, Rotta Loria et al. (2020) recommended $\psi_0 = 0.60$, $\psi_1 = 0.50$ and $\psi_2 = 0.50$ for the combination, frequent and quasi-permanent values of variable actions, respectively. Regarding the consideration of thermal loads during cooling of the building side (i.e. temperature increase along the energy piles), two design combinations must be considered, assuming the effects of the thermal loads make them the dominant load ($\Delta T_k = Q_{k,1}$, where $Q_{k,1}$ is the dominant variable load) or if not ($\Delta T_k = Q_{k,i}$, where $Q_{k,i}$ is the i^{th} general variable load), since it is not known if the thermal loads are dominant with respect to the mechanical ones. Regarding the heating of the building side (i.e., temperature decrease along the energy piles) a single design combination must be considered ($\Delta T_k = Q_{k,1}$).

Finally, when the influence of thermal loads is analyzed during the design of energy piles, (i) piles free at the head and (ii) piles that are fully restrained should be considered to attain conservative estimations of vertical displacement and stress, respectively.

5. CONCLUSIONS

The fundamental research in the field of energy geostructures, compiled and expanded by the Laboratory of Soil Mechanics over more than two decades, revealed that this emerging technology provides low carbon, cost-effective and local energy solutions to structures and infrastructures, which opens a new era for the geotechnical engineering practice.

The research activities performed by LMS in this field has exclusively covered various elements related to energy geostructures, including but not limited to energy, geotechnical, structural and design aspects. Related to the energy aspect, it has been revealed that typically, 40-150 W/m heat energy can be extracted from and withdrawn into the ground with the use of energy piles, while 20-40 W/m^2 and 20-60 W/m^2 are achievable with energy wall and energy tunnels, respectively. Furthermore, two state-of-the-art in-situ tests have been performed on single and a group of energy piles, which not only revealed the most fundamental knowledge regarding their thermo-mechanical behavior, but also provided invaluable information for the validation of numerical models and analytical tools developed in the area.

To provide satisfactory tools for design and wider application of energy piles, several practical analytical tools have been developed for energy piles including the load-transfer method for the assessment of axial stress, displacement and mobilized shaft resistance along single and groups of energy piles, as well as the interaction factor method for the estimation of vertical displacement of energy pile groups with and without a rigid slab. Incremental research efforts performed in the area, from both experimental and analytical points of view, have eventually led to development of recommendations for the design of energy piles for both ultimate and serviceability limit states. Overall, research outcomes achieved over more than two decades revealed that the energy geostructures concept is a mature and ready-to-be-employed technology.

The questions that remained to be answered now are no longer about how an energy geostructure responds to thermal actions, but rather on how the energy performance, as well as the geotechnical and structural adaptations should be assessed to maximize its cost efficiency.

ACKNOWLEDGEMENT

The financial supports from the Swiss National Science Foundation N. 160117 (Division IIII), Swiss National Science Foundation N. 200021_175500 (Division II), Swiss Federal Office of Energy (contract Nb. 154'426) are greatly appreciated.

REFERENCES

[1] A. Bidarmaghz and G. A. Narsilio: Heat exchange mechanisms in energy tunnel systems. Geomechanics for Energy and the Environment, 16, 83-95, 2018.

[2] A. Di Donna et al: Energy performance of diaphragm walls used as heat exchangers. Proceedings of the Institution of Civil Engineers-Geotechnical Engineering, 170(3), 232-245, 2017

[3] A. F. Rotta Loria: Performance-based design of energy pile foundations. DFI Journal 12 (2), 94-107, 2019.

[4] A. F. Rotta Loria et al: The role of thermal loads in the performance-based design of energy piles. Geomechanics for Energy and the Environment, 21, 100153, 2020.

[5] A. F. Rotta Loria and L. Laloui: The interaction factor method for energy pile groups. Computers and Geotechnics, 80, 121-137, 2016.

[6] A. F. Rotta Loria and L. Laloui: Thermally induced group effects among energy piles. Géotechnique, 67(5), 374-393, 2017.

[7] A. F. Rotta Loria and L. Laloui: Group action effects caused by various operating energy piles. Géotechnique, 68(9), 834-841, 2018.

[8] ASHRAE 2008: ASHRAE Vision 2020. https://www.isiaq.org/docs/sponsor%20material/ASHRAE%20Strategic%20Plan%20Jun08.pdf. Last accessed June 2024.

[9] C. Knellwolf et al : Geotechnical analysis of heat exchanger piles. Journal of Geotechnical and Geoenvironmental Engineering, 137(10), 890-902, 2011.

[10] C. Xia et al: Experimental study on geothermal heat exchangers buried in diaphragm walls. Energy and Buildings. 52, 50-5, 2012.

[11] D. Adam and R. Markiewicz: Energy from earth-coupled structures, foundations, tunnels and sewers. Géotechnique, 59(3), 229-236, 2009.

[12] D. P. Nicholson et al: The design of thermal tunnel energy segments for Crossrail, UK. Proceedings of the Institution of Civil Engineers Engineering Sustainability, 167 (3), 118-134, 2014.

[13] D. Salciarini et al: Thermomechanical effects induced by energy piles operation in a small piled raft. International journal of Geomechanics, 15(2), 04014042, 2013.

[14] D. Sterpi et al: Investigation on the behaviour of a thermo-active diaphragm wall by thermo-mechanical analyses. Geomechanics for Energy and the Environment, 9, 1-20, 2017.

[15] E. M. Comodromos et al : Contribution to the design methodologies of piled raft foundations under combined loadings. Canadian Geotechnical Journal, Vol. 53 (4), 559–577, 2016.

[16] E. P. B. D. Recast: Directive 2010/31/EU of the European Parliament and of the Council of 19 May 2010 on the energy performance of buildings (recast). Official Journal of the European Union 18, no. 06, 2010.

[17] E. Ravera et al : Analysis of the interaction factor method for energy pile groups with slab. Computers and Geotechnics, Vol 119, 2019.

[18] E. Ravera et al: Load-transfer method for energy piles in a group with pile-soil-slab-pile interaction. Journal of Geotechnical and Geoenvironmental Engineering, Vol 146 (6), 2020.

[19] E. Sailer et al: Fundamentals of the coupled thermo-hydro-mechanical behaviour of thermo-active retaining walls. Computers and Geotechnics, 109, 189-203, 2019.

[20] Eurostat, (2022): https://ec.europa.eu/eurostat/statistics-explained/index.php?title=Energy_consumption_in_households (last accessed June 2024)

[21] F. A. Loveridge et al: Long-term monitoring of CFA energy pile schemes in the UK. Energy Geotechnics, 585-592, 2016.

[22] H. B. Seed and L. C. Reese: The action of soft clay along friction piles. American Society of Civil Engineers Society, 122 (1), 731–754, 1957.

[23] H. G. Poulos: Analysis of the settlement of pile groups. Géotechnique, 18 (4), 449-471, 1968.

[24] H. G. Poulos: The influence of a rigid pile cap on the settlement behaviour of an axially-loaded pile. Civ. Eng. Trans., Inst. Engrs, CE10 (2), 206-208, 1968.

[25] H. M. Coyle and L. C. Reese: Load transfer for axially loaded piles in clay. J. Soil Mech. Found. Div. ASCE. 92 (2), 1–26, 1966.

[26] International Energy Agency, I. E. A. 2022: Heating, https://www.iea.org/energy-system/buildings/heating#tracking (Last accessed June 2024).

[27] International Energy Agency, I. E. A. 2018: https://www.iea.org/reports/the-future-of-cooling (last accessed June 2024)

[28] J. S. McCartney and K. D. Murphy. Investigation of potential dragdown/uplift effects on energy piles. Geomechanics for Energy and the Environment, 10, 21-28, 2017.

[29] L. Laloui et al: Comportement d'un pieu bi-fonction, fondation et échangeur de chaleur. Canadian Geotechnical Journal, 40(2), 388-402, 2003.

[30] L. Laloui et al: Experimental and numerical investigations of the behaviour of a heat exchanger pile. International Journal for Numerical and Analytical Methods in Geomechanics, 30(8), 763-781, 2006.

[31] L. Laloui and A. F. Rotta Loria. Analysis and Design of Energy Geostructures: Theoretical Essentials and Practical Applications. Academic Press, 2019.

[32] L. Laloui and M. Sutman: Experimental investigation of energy piles: From laboratory to field testing. Geomechanics for Energy and the Environment, 27, p.100214, 2021.

[33] L. Laloui et al: Issues involved with thermoactive geotechnical systems: characterization of thermomechanical soil behavior and soil-structure interface behavior. DFI Journal-The Journal of the Deep Foundations Institute, 8(2), pp.108-120, 2014.

[34] L. M. Kraft et al: Theoretical T-Z curves. Journal of Geotechnical Engineering, American Society of Civil Engineers, 107 (11), 1543–1561, 1981.

[35] M. Barla and A. Di Donna: Energy tunnels: concept and design aspects. Underground Space, 3(4), 268-276, 2018.

[36] M. Barla et al: A novel real-scale experimental prototype of energy tunnel. Tunnelling and Underground Space Technology, 87, 1-14, 2019.

[37] M. F. Randolph and P. Clancy: Efficient design of piled rafts. Proceedings of 5th International Conference on Deep Foundations on Bored and Auger Piles, 1-4 June, Ghent, Belgium, 119-130, 1993.

[38] M. F. Randolph and C. P. Wroth: Analysis of deformation of vertically loaded piles. Journal of Geotechnical Engineering, American Society of Civil Engineers, 104 (2), 1465–1488, 1978.

[39] M. Sutman et al: Full-scale in-situ tests on energy piles: Head and base-restraining effects on the structural behaviour of three energy piles. Geomechanics for Energy and the Environment, 18, 56-68, 2019.

[40] M. Sutman et al: Effect of end-restraint conditions on energy pile behavior. Geotechnical Frontiers, 165–174, 2017.

[41] M. Sutman et al: Cyclic Load–Transfer Approach for the Analysis of Energy Piles. Journal of Geotechnical and Geoenvironmental Engineering, 145(1), 04018101, 2018.

[42] M. Sutman et al: Long-term performance and life cycle assessment of energy piles in three different climatic conditions. Renewable Energy, 146, 1177-1191, 2020.

[43] M. Sutman: Thermo-mechanical behavior of energy piles: Full-scale field testing and numerical modeling (Doctoral dissertation, Virginia Tech), 2016.

[44] N. Makasis et al: A machine learning approach to energy pile design. Computers and Geotechnics, 97, 189-203, 2018.

[45] P. J. Bourne-Webb et al : Energy pile test at Lambeth College, London: geotechnical and thermodynamic aspects of pile response to heat cycles. Géotechnique, 59(3), 237-248, 2009.

[46] P. J. Bourne-Webb et al: Thermal and mechanical aspects of the response of embedded retaining walls used as shallow geothermal heat exchangers. Energy and Buildings, 125, 130-141, 2016.

[47] P. J. Bourne-Webb et al: Design tools for thermoactive geotechnical systems. The Journal of the Deep Foundations Institute, 8(2), 121-129, 2014

[48] R. Frank and S. R. Zhao: Estimation par les paramètres pressiométriques de l'enfoncement sous charge axiale de pieux forés dans des sols fins. Bulletin de Liaison Laboratoires des Ponts et Chaussees, No. 119, 17–24, 1982.

[49] S. Frodl et al: Design and construction of the tunnel geothermal system in Jenbach. Geomechanics and Tunnelling, 3(5), 658-668, 2010.

[50] S. Kürten, S et al: Design of plane energy geostructures based on laboratory tests and numerical modelling. Energy and Buildings, 107, 434-444, 2015.

[51] S. You et al: Experimental study on structural response of CFG energy piles. Applied Thermal Engineering, 96, 640-651, 2016.

[52] T. Mimouni, L. Laloui: Behaviour of a group of energy piles. Canadian Geotechnical Journal, 52(12), 1913-1929, 2015.